Pergamon

Journal of Structural Geology, Vol. 19, Nos 3–4, pp. 269 to 278, 1997

0191-8141/97 $17.00 + 0.00

PII: S0191-8141(96)00095-8

A kinematic model for the formation of duplex systems with a perfectly planar roof thrust

JUAN CONTRERAS* and MAX SUTER†

Instituto de Geología, Universidad Nacional Autónoma de México (UNAM), Apartado Postal 70-296, C.P. 04510, Ciudad de México, Distrito Federal, Mexico

(*Received* 1 *February* 1996; *accepted in revised form* 15 *October* 1996)

Abstract—We present a cross-sectional kinematic forward model for the formation of duplexes with a perfectly planar roof thrust. The major assumptions are a constant dip and constant spacing of the ramps in the undeformed state and sequential deformation in the direction of tectonic transport, with equal displacement along each ramp. The model is based on a coordinate transformation that simulates flexural slip parallel to the active fault surface. This causes angular parallel folds and keeps the layer thickness constant, except in the forelimbs of the horses. Attempts by previous workers to simulate the formation of duplexes with a perfectly planar roof thrust, on the other hand, were based on the assumptions of constant bed thickness and bed length, or a different topology of the axial planes delimiting the forelimbs of the horses, and resulted in corrugated roof thrusts. We show that it is not possible to form a flat roof duplex type and preserve the forelimb thickness of the horses under flexural slip parallel to the active fault. We describe duplexes by three parameters which are the separation s between ramps, the ramp length l, and the displacement u along the ramps. In a u/s vs l/s diagram, duplexes with a perfectly planar roof thrust, resulting from numerical experiments with our kinematic algorithm, occupy specific families of straight lines. Our results are independent of the dip or internal geometry of the thrust ramps.

INTRODUCTION

Duplex structures provide a mechanism for slip transfer from a layer-parallel glide horizon at depth (floor thrust) to another at a shallower stratigraphic level (roof thrust) (Boyer and Elliott, 1982). Duplexes are blind thrust systems; the roof thrust is contained within the stratigraphic section and does not reach the surface. Slip transfer is sequential in the direction of tectonic transport and occurs along a system of footwall ramps (called ramps in this paper) that cut across the stratigraphic layering and link the floor and roof thrusts (Fig. 1). As each new ramp forms, the previous imbricate fault is deactivated and carried passively within the enclosing thrust sheet (Boyer and Elliott, 1982; Mitra and Boyer, 1986). Displacement along each ramp is minor compared to that on the floor and roof thrusts.

Natural duplex structures have been observed on various length scales in fold–thrust belts and often have a planar roof thrust (for example Elliott and Johnson, 1980; Boyer and Elliott, 1982; Mitra, 1986; Mitra and Boyer, 1986; Tanner, 1992). Groshong and Usdansky (1988) and Cruikshank *et al.* (1989) attempted to simulate the formation of duplexes with a planar roof thrust. However, their models, which were based on the assumptions of constant bed thickness and bed length or a different topology of the axial planes delimiting the forelimbs of the horses, resulted in corrugated roof thrusts. We previously presented a kinematic model, based on a coordinate transformation, that simulates flexural slip parallel to an active fault surface (Contreras and Suter, 1990) and made numerical experiments with an algorithm (Contreras, 1991) that is based on this kinematic model. These experiments showed that our

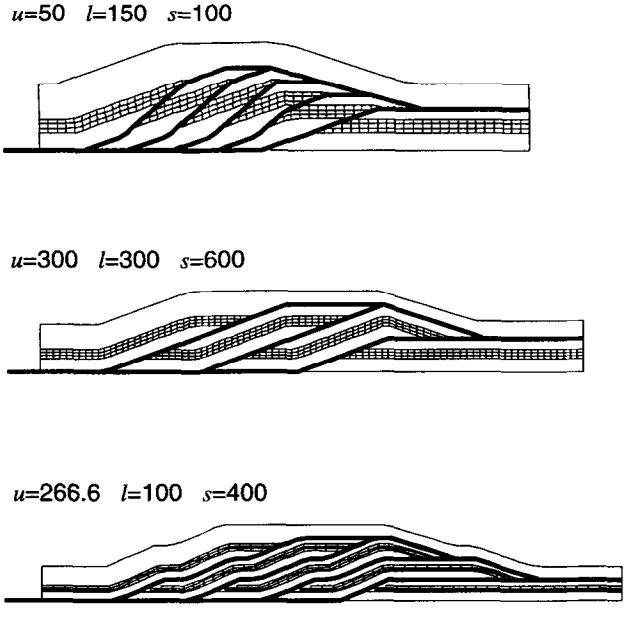

Fig. 1. Examples of duplexes with a planar roof thrust modeled with a kinematic algorithm that assumes displacement of constant length, parallel to the underlying active fault segment, for all the displaced particles throughout the medium (Fig. 2). For the definition of the duplex parameters (u: displacement along the ramps, l: ramp length, and s: separation between the ramps in the undeformed state) see Fig. 3. The ramp series has a constant dip and spacing in the undeformed state, and the deformation sequence is in the direction of tectonic transport, with equal displacement along each ramp.

*Present address: Lamont-Doherty Earth Observatory of Columbia University, P.O. Box 1000, RT 9W, Palisades, NY 10964, U.S.A.

†Present address: Instituto de Geología, Universidad Nacional Autónoma de México (UNAM), Estación Regional del Noroeste, Apartado Postal 1039, C.P. 83000 Hermosillo, Sonora, Mexico

model is capable of simulating the formation of duplexes with a perfectly planar roof thrust (Fig. 1).

It is the purpose of this paper to analyze in more detail under what conditions our kinematic model simulates duplex systems with a planar roof thrust. For that purpose we define a parameterization of duplex structures. We then investigate by computer experiments with our algorithm, as well as analytically, where in this parameter-space duplex structures with a planar roof thrust form. Eventually, we discuss why attempts by other authors failed to simulate duplex structures with a planar roof thrust. First, however, we shall summarize the characteristics of the kinematic model used in our simulation of duplex structures.

KINEMATIC MODEL

The kinematic model used in this paper for the simulation of duplex structures was introduced by Contreras and Suter (1990). Our model only applies to regions being deformed by shortening or extension, whereas natural duplex systems have also been observed in regions being deformed by strike-slip (Twiss and Moores, 1992). Furthermore, the model is two-dimensional and limited to the cross-sectional geometry of duplexes. It is based on a coordinate transformation to a more deformed state and is formulated analytically in terms of the less deformed configuration (forward modeling, Lagrangian description). The medium is subdivided into homogeneous displacement vector fields that are delimited by the planes bisecting the fault inflections (Fig. 2). The displacement trajectory is of constant length for all the displaced particles throughout the medium and parallel to the underlying active fault segment (Fig. 2). Consequently, the deformation path is continuous but not smooth and causes an angular style of parallel folding, except in the forelimb of the resulting fold (area to the right of axial plane III in Fig. 3a) where the layer thickness is not conserved (see Appendix). Our model also considers an external component of fault-parallel simple shear (Fig. 2) that is uniformly distributed throughout the hanging wall. The transformation can be expressed as

$$\begin{bmatrix} p'_x \\ p'_y \\ 1 \end{bmatrix} = \begin{bmatrix} 1 & 0 & -l_x \\ 0 & 1 & -l_y \\ 0 & 0 & 1 \end{bmatrix} \times \begin{bmatrix} \cos\alpha & -\sin\alpha & 0 \\ \sin\alpha & \cos\alpha & 0 \\ 0 & 0 & 1 \end{bmatrix} \times \begin{bmatrix} 1 & 0 & l_x \\ 0 & 1 & l_y \\ 0 & 0 & 1 \end{bmatrix} \times \begin{bmatrix} p_x + u + h\tan\psi \\ p_y \\ 1 \end{bmatrix}, \quad (1)$$

where the left side of the equation represents the coordinates in the deformed state. The first three matrices on the right side of the equation represent a rigid-body rotation around the intersection of the rigid-body displacement path with the axial plane a (rotation **R** in Fig. 2), and the vector on the right side of the equation represents shearing and rigid-body translation. Expanding equation (1), the general expression that controls the displacement u of a particle p parallel to a given fault segment (Fig. 2) becomes

$$\begin{aligned} p'_x &= (p_x + u + h\tan\psi)\cos\alpha \\ &\quad - [p_y + f_x\cot(\alpha/2) - f_y](1 - \cos\alpha)\tan(\alpha/2) \\ p'_y &= p_y + (p_x + u + h\tan\psi)\sin\alpha \\ &\quad + [p_y + f_x\cot(\alpha/2) - f_y]\sin\alpha\,\tan(\alpha/2), \end{aligned} \quad (2)$$

where p_x, p_y and p'_x, p'_y (Fig. 2) are the coordinates of the particle before and after the transformation, respectively, h is the distance of the particle from the fault, ψ is the angle of external simple shear applied to the hanging wall (clockwise increases of ψ are considered positive), α is the change in dip of the fault at the inflection (counterclockwise changes of α are considered positive), and f is the point of intersection between the fault inflection and the corresponding axial plane (Fig. 2). A complete

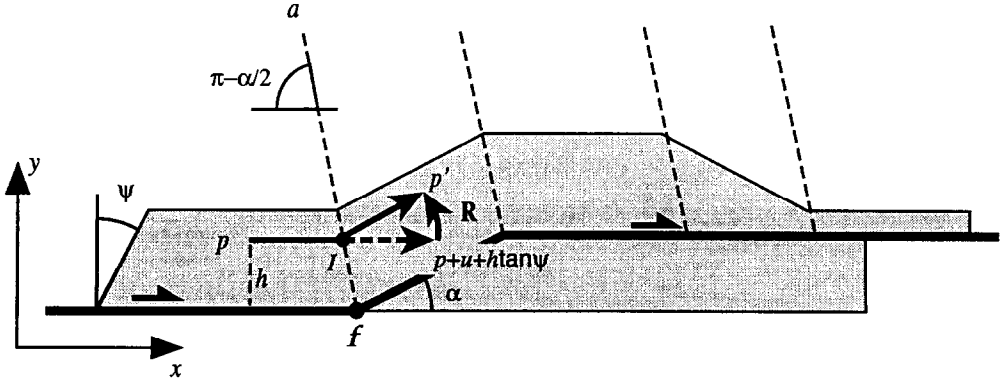

Fig. 2. Configuration and parameters of the kinematic forward model used in the simulation of the duplex structures (from Contreras and Suter, 1990). The model is based on a coordinate transformation that simulates flexural slip parallel to the active fault surface. Note that the axial planes delimiting the forelimb of the fault-related fold do not bisect the dip domains of the hanging wall, but are parallel to the plane bisecting the fault inflection between the ramp and the roof thrust. This results from our constraint that the displacement vectors be of constant length and parallel to the underlying fault. Further explanations in the text.

derivation of equations (1) and (2) from first principles is provided in Contreras and Suter (1990). A more general formulation of these operations, which are common in computer graphics (for example Foley and van Dam, 1982), has recently been presented by De Paor (1994).

The inhomogeneity of the displacement vector field across axial planes introduces longitudinal and angular shear strains. An analysis of this strain is provided in Contreras and Suter (1990) and summarized in the Appendix. Furthermore, it can be shown that the defined transformations do not cause a change in area; the deformation is isochoric, which is typical of deformation by simple shear (Truesdell and Toupin, 1960).

DUPLEX STRUCTURES WITH A PLANAR ROOF THRUST

In our kinematic model for the formation of duplex structures with a planar roof thrust we assume that all the ramps have the same dip in the undeformed state and that the deformation is sequential in the direction of tectonic transport (Figs 1 & 3). This is based on the observation that ramps of natural duplexes often have a constant dip (Tanner, 1992), and sequential deformation in the direction of tectonic transport is characteristic of duplex structures (Boyer and Elliott, 1982).

We first examine general cases of duplex systems, where the spacing of the ramps varies, and analyze the displacement conditions that lead to a planar roof thrust. We then analyze duplex systems with a regular ramp spacing and equal displacement along each ramp and derive a general expression for the formation of a planar roof thrust under these specific conditions. This is justified, as the ramps of natural duplexes often have a regular spacing that is linearly related to the thickness of strata involved in the duplex (Liu and Dixon, 1995). No external simple shear is applied during the formation of our duplex models; consequently ψ vanishes from equation (2).

We describe duplexes by three parameters: the separation s between ramps in the undeformed state (measured parallel to the floor thrust), the ramp length l in the undeformed state, and the displacement u along the ramps (Fig. 3a). (Also marked on Fig. 3 is the dip α of the ramps. However, as we will see below, the formation of duplex systems with a planar roof thrust is independent of the ramp dip.) Furthermore, we combine these three variables into the two non-dimensional parameters l/s and u/s, which permits characterization of any duplex by these three variables in a two-dimensional space (Fig. 4).

We also use in this paper the following conventions: displacements are considered small where $u < l$ and large where $u > l$. In our equations, duplexes with a planar roof thrust, small displacements, and n horses are coded $d(n)$, whereas duplexes with a planar roof thrust, large displacements and n horses are coded $D(n)$. The number of horses n is defined as the minimum number of horses required to form a planar roof thrust. For example, in the duplexes of Fig. 1, the minimum number of horses required to form a planar roof thrust is, from top to bottom, four, two, and three. A similar labeling system is also used for duplexes with a corrugated roof thrust on Fig. 4, where $r(n)$ stands for a duplex with n horses and small displacements and $R(n)$ for a duplex with n horses and large displacements.

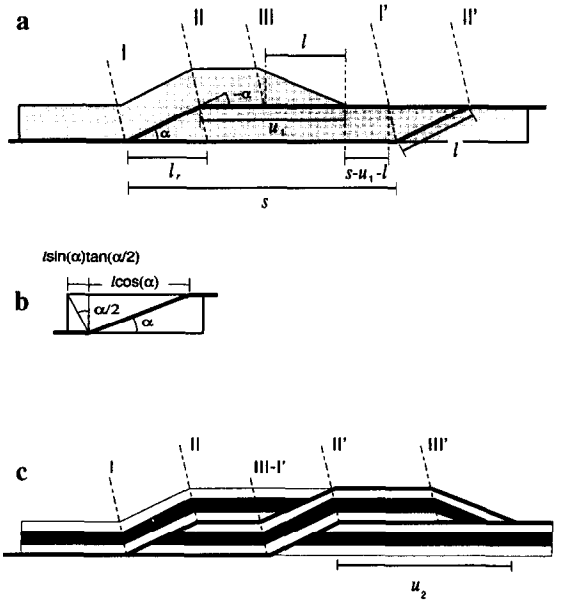

Fig. 3. Formation of a duplex with a planar roof thrust and two horses for large displacements: (a) Parameters used in the description of duplex systems are the separation s between the ramps in the undeformed state (measured parallel to the floor thrust), the dip α and length l of the ramps in the undeformed state, and the displacement u_1 along the first ramp. The displacement u_1 along the ramp is large ($u_1 > l$). (b) Geometric relation used in the derivation of equation (4). (c) Final deformed geometry of the duplex. The constant dip of the ramps causes the axial planes to be parallel. A planar roof thrust results when the axial planes III and I' are identical, which is the case when the sum of the displacements along the two ramps equals their separation (equation 4).

Mitra and Boyer (1986) introduced a duplex classification, which is based on a comparison between u and s: according to these authors, for $u < s$ the duplex is hinterland dipping, for $u = s$ the structure is an antiformal stack, and for $u > s$ the duplex is foreland dipping. We adopt the duplex classification by Mitra and Boyer (1986), but will define below different parameter ranges for these three classes of duplexes.

Duplex structures with two horses and large displacements (u > l)

Consider a simple ramp of length l that forms an angle α with the upper and lower detachments and a large displacement $u_1 > l$ along the ramp (Fig. 3a). After the displacement, the medium forms a fault-related fold.

Note that the axial planes delimiting the forelimb do not bisect the dip domains of the hanging wall, but are parallel to the plane bisecting the fault inflection between the ramp and the roof thrust. This results from our constraint that the displacement vectors be of constant length and parallel to the underlying fault. Consider now a new ramp with the same geometry as the first one (Fig. 3c). To form a duplex with a planar roof thrust, it is necessary to transport the axial plane (III) along the detachment segment of the new fault until it coincides with the axial plane (I'). This occurs when the displacement u_2 satisfies the condition

$$u_2 = s - (u_1 + l_r) + l \qquad \text{for } u_2 > l, \tag{3}$$

where $l_r = l\sin\alpha\tan(\alpha/2) + l\cos\alpha$ (Fig. 3b).

Using the trigonometric identities:

$$\sin\alpha = 2\sin(\alpha/2)\cos(\alpha/2)$$

and

$$\cos\alpha = \cos^2(\alpha/2) - \sin^2(\alpha/2),$$

it can be demonstrated that $l_r = l$, therefore equation (3) can be expressed as

$$u_1 + u_2 = s \qquad \text{for } u_1, u_2 > l. \tag{4}$$

In the special case of equal displacements $u_1 = u_2 = u$, equation (4) reduces to

$$D2 \qquad \{u/s = 1/2 \qquad \text{for } u/s > l/s. \tag{5}$$

This configuration is a vertical line in the u/s vs l/s diagram on Fig. 4, where it is labeled *D2*. The condition that the displacement has to be twice the size of the separation between the two ramps in order to form a duplex system with a planar roof thrust was already recognized, if not derived mathematically, by Mitra and Boyer (1986). An increase in shortening ($u/s > 1/2$) results in a duplex with a corrugated roof thrust and a three-fold repetition of the stratigraphic sequence (region *R3* in Fig. 4). If we decrease the shortening ($u/s < 1/2$), our kinematic model generates a duplex system with a corrugated roof thrust and a two-fold repetition of the stratigraphic sequence (region *R2* in Fig. 4).

We now analyze the planarity of the roof thrust in our duplex model in terms of strain analysis. From equation (A3), it follows that the hanging wall ramp (base of the forelimb) of the first fault-related fold (l on Fig. 3a), to the right of the axial plane (III), does not become elongated, as its orientation is parallel to the transport direction. Therefore, the hanging wall ramp is accommodated on the backlimb of the consecutively formed fold without any corrugation. Furthermore, Fig. 3(a) shows that the hanging wall ramp of the first formed horse passes through two fault inflections. As both ramps have the same geometry, the two inflections only differ in sign, such that $\alpha_2 = -\alpha_1$, $\gamma_T = 0$, and $\Sigma\alpha_i = 0$ in equations (A2) and (A4), respectively, if no external simple shear is applied to the hanging wall ($\psi = 0$). Consequently, the quadratic elongation in equation (A1) reduces to $\lambda = 1$ (case of no elongation). Moreover, from equation (A4) it follows that the orientation of an arbitrary material line, after having passed through these two fault inflections, remains the same as in the undeformed state ($\delta' = \delta$).

From equation (3) and Fig. 3 we can also infer that structures with horses that are not imbricated (represented in Fig. 4 by the region labeled *B*) are formed when

$$l/s < 1 - 2u/s, \tag{6}$$

whereas structures with overlapping horses (duplexes and antiformal stacks) form for l/s ratios larger than this value. On the u/s vs l/s diagram (Fig. 4) the limit between the regions representing these two major types of structures is marked by a line in the lower left part of the diagram.

Duplex structures with two horses and small displacements ($u < l$)

Systems in the undeformed state with the geometry of Fig. 3, but a small displacement $u_1 < l$ along the first ramp, form in the deformed state a duplex with a planar roof thrust (Fig. 5) if the displacement u_2 satisfies the condition

$$u_2 = s - l \qquad \text{for } u_2 < l \tag{7}$$

or, in the special case of equal displacements $u_1 = u_2 = u$, the condition

$$d2 \qquad \{u/s + l/s = 1 \qquad \text{for } u/s < l/s. \tag{8}$$

This configuration is a straight line with a slope of (-1) in the u/s vs l/s diagram in Fig. 4, where it is labeled *d2*. Based on similar reasoning as in the former case (where $u/s > l/s$), it can easily be shown that the roof thrust of this duplex system is not corrugated.

In the case of $u/s + l/s < 1$, the two horses of the duplex system are partly imbricated and the roof thrust does become corrugated. This configuration is labeled *r2* in Fig. 4. In the case of $u/s + l/s > 1$, the final configuration is a hinterland-dipping duplex with a corrugated roof thrust, and three horses are required until the duplex system stops growing vertically. This type of structure is shown on Fig. 4 with the label *r3*.

Duplex structures with more than two horses

Synthetic duplex systems with more than two horses, created with our kinematic algorithm, can also develop planar roof thrusts (Fig. 1). We first deal with the case of a duplex with three horses and then derive a general expression for duplexes with n horses. Figure 6 illustrates the formation of a duplex with three horses and small displacements ($u < l$). For simplicity we consider the special case of a duplex system with a smooth front (without step). Figure 6(a) shows this configuration at the

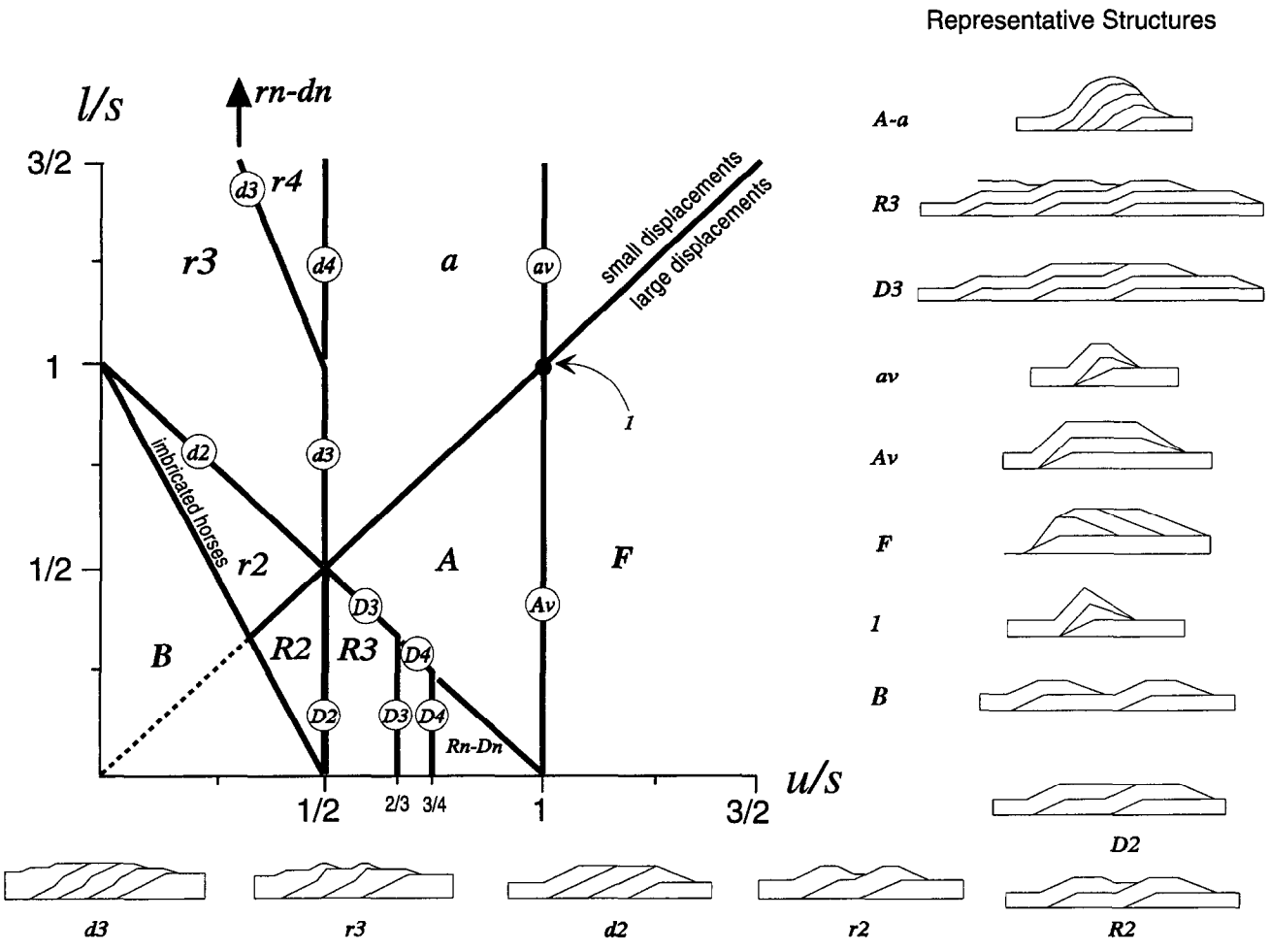

Fig. 4. Location of duplexes in a u/s vs l/s diagram and representative structures. Duplexes with a planar roof thrust and n horses are labeled $d(n)$ for small displacements ($u < l$) and $D(n)$ for large displacements ($u > l$). Similarly, duplexes with a corrugated roof thrust and n horses are labeled $r(n)$ for small displacements and $R(n)$ for large displacements. Antiformal stacks are located in the area labeled a–A (A represents the region below and a the region above the line separating large from small displacements), and foreland-dipping duplexes in the region labeled F. Antiformal stacks with vertical growth are located on the line labeled Av–av (Av represents the segment below and av above the line separating large from small displacements), and the point marked l represents the special case of an antiformal stack with a chevron geometry. The region labeled B corresponds to duplexes with horses that are not imbricated. Further explanations in the text.

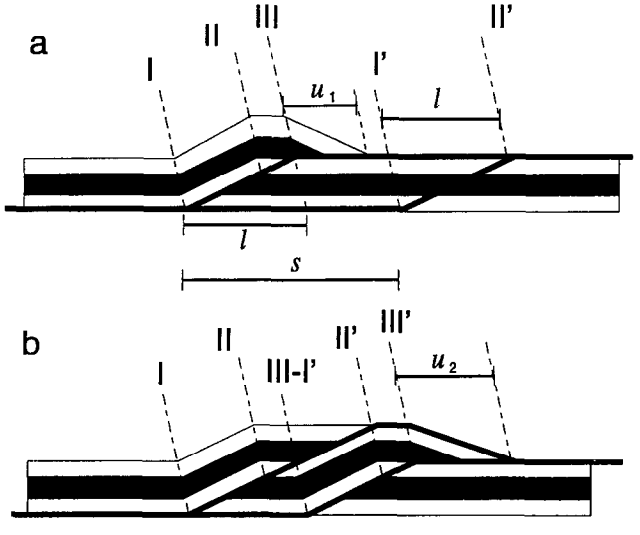

Fig. 5. Formation of a duplex with a planar roof thrust for the case of two horses and small displacements ($u < l$). (a) Geometry after execution of the displacement u_1. (b) Final deformed geometry of the duplex. This type of structure is characterized by equation (8) and its location in Fig. 4 is labeled *d2*.

stage when a displacement u_1 has occurred along the first ramp such that a part of the hanging wall has moved to the right of axial plane (I'). Figure 6(b) shows the geometry of this structure after the occurrence of the displacement u_2 along the second ramp. To form a three-horse duplex with a smooth front, it is necessary that

$$u_2 = s_1 - u_1. \tag{9}$$

To obtain a duplex with a planar roof thrust (Fig. 6c), the displacement u_3 has to become

$$u_3 = u_1 - (s_1 - l). \tag{10}$$

The front of the hanging wall is also smooth if u_3 fulfills the condition

$$u_3 = s_2 - u_2. \tag{11}$$

Combining equations (9) to (11) and assuming equal displacements $u = u_1 = u_2 = u_3$ and equal spacing $s = s_1 = s_2$, we obtain the general expression for duplexes

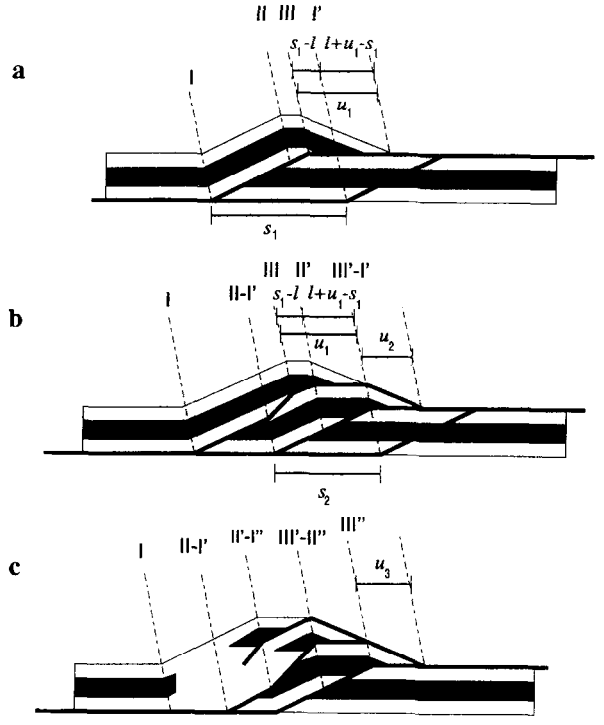

Fig. 6. Kinematic sequence showing the formation of a duplex with a planar roof thrust for the case of three horses and small displacements ($u<l$). The planar roof thrust only forms after the imbrication of the third horse in Fig. 6(c). This type of structure is characterized by equations (12) and its location in Fig. 4 is labeled *d3*.

that have a planar roof thrust, are composed of three horses, and have small displacements along their ramps:

$$d3 \quad \begin{cases} u/s = 1/2 \\ u/s + l/2s = 1 \end{cases} \qquad \text{for } u/s < l/s \text{ and } n = 3. \tag{12}$$

Numerical experimentation with our kinematic algorithm confirms that duplexes with geometric and kinematic parameters satisfying either one of these two equations develop a planar roof thrust. In Fig. 4 this type of structure is located on two straight line segments labeled *d3*.

We now deal with the case of a duplex with three horses and large displacements ($u>l$). A special case of this structural configuration is shown in Fig. 7, where u and s are constant. This structure forms when the axial planes II and I' coincide (Fig. 7b), which occurs when the displacement $u=s-l$ for $u>l$, or equivalently

$$u/s + l/s = 1 \qquad \text{for } u/s > l/s. \tag{13}$$

A second condition can be derived, based on the observation that $u=2s/3$ for $u>l$ (Fig. 7a) or

$$u/s = 2/3 \qquad \text{for } u/s > l/s. \tag{14}$$

Combining equations (13) and (14), we obtain the general expression for duplexes with three horses, a planar roof thrust, and large displacements along their ramps:

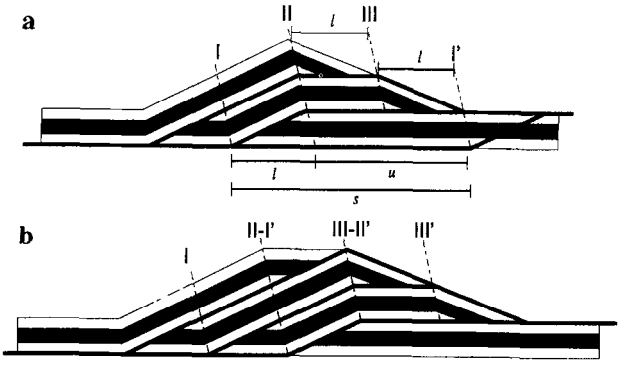

Fig. 7. Kinematic sequence showing the formation of a duplex with a planar roof thrust for the case of three horses and large displacements ($u>l$). The roof thrust only becomes planar after the imbrication of the third horse (Fig. 7b). This type of structure is characterized by equations (15) and its location in Fig. 4 is labeled *D3*.

$$D3 \quad \begin{cases} u/s = 2/3 \\ u/s + l/s = 1 \end{cases} \qquad \text{for } u/s > l/s \text{ and } n = 3. \tag{15}$$

These expressions describe, similarly to equation (12), two straight line segments labeled *D3* in Fig. 4.

We now generalize equations (5), (8), (12), and (15), which are valid for two and three horses, to formulate expressions for infinite series of duplexes, coded $d(n)$, with a planar roof thrust, n horses, and small displacements, as well as for infinite series of duplexes, coded $D(n)$, with a planar roof thrust, n horses, and large displacements. These series have to satisfy one of the following conditions:

$$d(n) \quad \begin{cases} u/s = 1/2 \\ u/s + l/[s(n-1)] = 1 \end{cases} \qquad \text{for } u/s < l/s, \tag{16a}$$

$$D(n) \quad \begin{cases} u/s = (n-1)/n \\ u/s + l/s = 1 \end{cases} \qquad \text{for } u/s > l/s. \tag{16b}$$

In these expressions, duplexes with a planar roof thrust and small displacements $d(n)$ are located on the vertical line $u/s=1/2$ and duplexes with large displacements $D(n)$ on the straight line $u/s+l/s=1$ (Fig. 4), regardless of their number n of horses.

A more detailed analysis is necessary to delimit the domain and co-domain of these equations. Separating l/s in equation (16a) and substituting $u/s=1/2$ we obtain

$$l/s = (n-1)/2, \tag{17}$$

where n is the minimum amount of horses required to form a duplex with a planar roof thrust. Equation (17) can be written as the sequence

$$l/s = 1/2,\ 1,\ 3/2, \ldots \qquad n = 1,\ 2,\ 3 \ldots. \tag{18}$$

This means that as we move upward along the vertical line $u/s=1/2$, n increases by 1 at each 1/2-interval of the

l/s-axis. Furthermore, $u/s=1/2$ bounds $u/s+l/[s(n-1)]=1$. Therefore, the co-domain of equation (16a) can be delimited as follows:

$$d(n)\begin{cases} u/s = 1/2 & \text{for } (n-1)/2 \geq l/s > (n-2)/2 \\ u/s + l/[s(n-1)] = 1 & \text{for } 1/2 > u/s > 0. \end{cases} \quad (19)$$

Similarly, in equation (16b) the straight line $u/s+l/s=1$ is piecewise continuous with respect to n, and each of these parts is limited by the sequence $u/s=(n-1)/n$, such that

$$D(n)\begin{cases} u/s = (n-1)/n & \text{for } 1/n \geq l/s > 0 \\ u/s + l/s = 1 & \text{for } (n-1)/n > u/s > (n-2)/(n-1). \end{cases} \quad (20)$$

Equations (19) and (20) are the general expressions that characterize duplexes with a planar roof thrust. Note that in equation (20) $u/s=(n-1)/n$ converges to 1 for very large values of n (where n is the minimum number of horses required to form a planar roof thrust). This number was already recognized by Mitra and Boyer (1986) as critical for the formation of antiformal stacks, which these authors define by $u=s$. As described above, these structures can contain an infinite number of horses, which implies that duplexes fulfilling this ratio only grow vertically, but not in width. This corresponds to the line labeled as *Av–av* in Fig. 4, where the corresponding structures are also illustrated (*Av* represents the segment below and *av* the segment above the line separating large from small displacements). Larger u/s ratios cause duplexes to dip in the foreland direction (region labeled *F* in Fig. 4).

The families of straight lines represented by equations (19) and (20) are located in the u/s vs l/s diagram in Fig. 4 to the left of the vertical line $u/s=1/2$ and below the line $u/s+l/s=1$ as well as on these two lines. This leaves a region in the diagram, to the right and above these two lines, which is additionally delimited by the region for foreland-dipping duplexes ($u/s>1$). This remaining area, labeled *a–A* (*A* represents the region below and *a* the region above the line separating large from small displacements), holds structures that we have not further explored, but which are probably best described as antiformal stacks. Examples of these structures are shown in Fig. 8. Therefore, rather than to consider antiformal stacks to be limited to the ratio $u/s=1$, as defined by Mitra and Boyer (1986), we propose that these structures are characterized by $1/2<u/s\leq 1$. It seems to us more plausible to define antiformal stacks by a range of u/s values, rather than the specific u/s value of 1, which is unlikely to be satisfied by natural duplexes. Note, however, that the lower limit of this range ($u/s=1/2$), which delimits antiformal stacks from hinterland-dipping duplexes, is defined arbitrarily. Some duplex models with this u/s ratio are shown in Fig. 9.

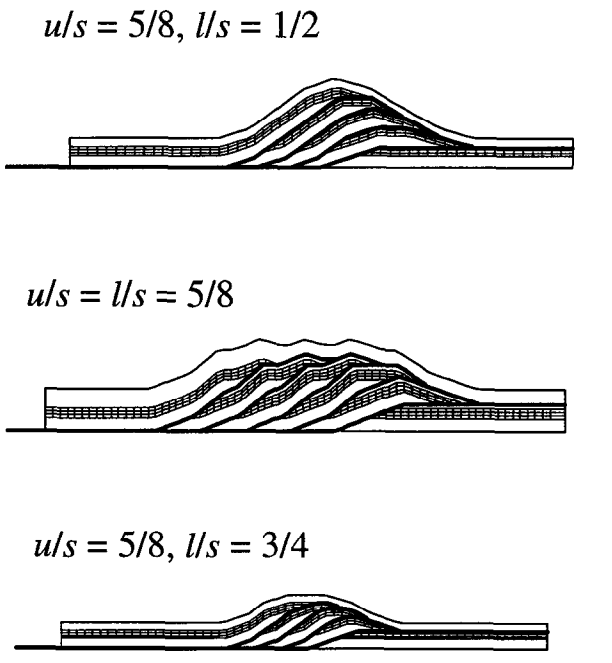

Fig. 8. Examples of duplex models with a u/s ratio of 5/8, corresponding to the region labeled *a–A* in the u/s vs l/s diagram on Fig. 4. These structures are probably best described as antiformal stacks, even though antiformal stacks, as originally defined by Mitra and Boyer (1986), are limited to the ratio $u/s=1$.

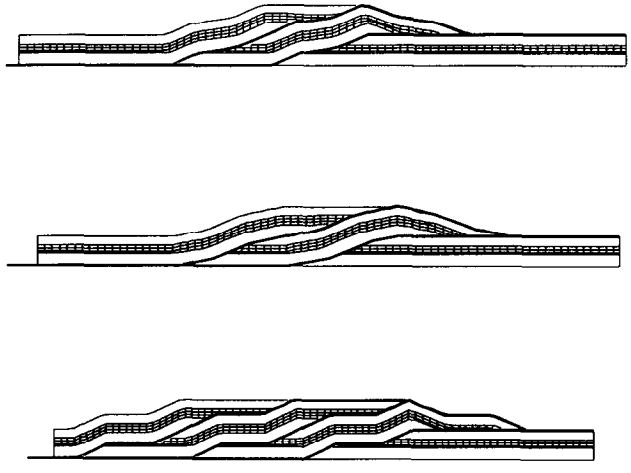

Fig. 9. Duplex structures with a planar roof thrust, modeled with our algorithm, where the thrust ramps are composed of various segments or have steps at several stratigraphic levels. The model parameters are $u/s=l/s=1/2$. The results indicate that the equations derived in this paper for the formation of duplexes with a planar roof thrust are independent of the ramp geometry. Further explanations in the text.

DISCUSSION

Many duplex simulations (for example Mitra, 1986; Groshong and Usdansky, 1988) are based on the fault-bend fold model introduced by Suppe and Namson (1979) and Suppe (1983) for the formation of folds above ramps. The model assumes conservation of bed length and bed thickness. These assumptions are approximated by the construction of symmetrical axial

surfaces that bisect the dip-domains in the backlimb (above the ramp) and in the forelimb of the resulting hanging wall fold. The shape of the forelimb is related to the dip of the ramp by trigonometric expressions with quadratic terms (Suppe, 1983). As a result, variations in the dip of the ramp are amplified in the dip of the forelimb of the hanging wall fold. This is crucial to the simulation of duplexes with a planar roof thrust, as in this case the forelimb cannot return to its initial state of orientation and distortion during passive translation along an underlying, subsequently active ramp. This explains why the duplex models by Groshong and Usdansky (1988), which are based on Suppe's approach, have a corrugated roof thrust, despite those authors' explicit intention to simulate duplexes with a planar roof thrust. The formation of a planar roof thrust in the duplex model by Boyer and Elliott (1982), a graphic experiment often referred to in the literature, is for the same reason kinematically not feasible. As explained above, no perfectly planar roof thrust can form in a duplex under flexural slip parallel to the active fault, if the original bed thickness remains preserved in the forelimbs of the horses.

Shi and Wang (1987), Johnson and Berger (1989), Cruikshank *et al.* (1989) and more recently Hardy (1995) have modeled fault-bend folds and duplexes in terms of domainal velocity distributions. Their models differ partly in the topology of the domain boundaries and in the velocity magnitudes assigned to the domains. Shi and Wang (1987) assume the horizontal velocity component to be constant within the hanging wall, whereas the velocity is assumed to be constant parallel to the fault surface in the models by Cruikshank *et al.* (1989), Johnson and Berger (1989) and Hardy (1995). In most of these models (for example, Cruikshank *et al.*, 1989), the velocity discontinuities are oriented such that originally horizontal beds experience no change in thickness or length as the thrust sheet moves over the ramp. For this reason these models produce the same fold shapes as the Suppe (1983) model and result in corrugated roof thrusts (Cruikshank *et al.*, 1989).

Our model is different from the ones mentioned above, which are not successful in simulating duplex systems with a planar roof thrust. Our formulation [equation (1)] is based on the superimposition of a vector displacement field and a strain field (Contreras and Suter, 1990). This model (Fig. 2) allows simulation of an external component of layer-parallel shear and furthermore quantifies the strain that occurs during the transformation across domain boundaries (see Appendix). These are major advantages compared to other models. For example, the representation of the medium by a mesh of quadrilateral elements permits the visualization of the distortion of the medium after the execution of these transformations for the grid nodes (Contreras and Suter, 1990). In our model, the axial planes delimiting the forelimb of the hanging wall fold are parallel to the plane bisecting the angle between the roof thrust and the ramp (Figs 2 & 3a). This satisfies our constraint that the slip vectors be of constant length and parallel to the underlying fault segment and leads to the formation of duplexes with a planar roof thrust (Fig. 1).

The equations derived in this paper for the formation of duplexes with a planar roof thrust are independent of the ramp geometry; the ramp dip α vanishes from the equations defining duplexes with a planar roof thrust. This is another difference to previous work, since most other models (for example Groshong and Usdansky, 1988) assume a specific ramp angle (typically 20–25°), and the results are therefore specific to that angle. Our model, on the other hand, is valid for any dip of the ramps and is independent of the ramp geometry. This is shown in Fig. 9, where we tested equations (19) and (20) for ramps that are composed of several segments or have steps at several stratigraphic levels. In these cases, the ramp length l is taken as the sum of the lengths of the individual segments. These duplex systems also form a planar roof thrust and have the same location in a u/s vs l/s diagram (Fig. 4) as duplexes with a simple ramp geometry.

It would have been interesting at this point to compare our models with published observations of natural duplex structures with a planar roof thrust. However, the fault network of natural duplexes is much less regular than in our idealization and there are variations in the amount of displacement between the individual horses. Furthermore, it is often not clear from published duplex sections how much of the structure is observed and how much is inferred, especially in the subsurface. Some planar roof thrusts are well documented, whereas the subsurface part of the corresponding sections is obviously much less constrained and its construction may be based on assumptions different from ours, such as constant bed length.

CONCLUSIONS

Duplexes can be characterized by three parameters which are the separation s between ramps, the ramp length l, and the displacement u. Foreland-dipping duplexes are characterized by $u/s > 1$, hinterland-dipping duplexes by $u/s < 1/2$, and antiformal stacks by $1/2 < u/s \leq 1$ (Fig. 4). This modifies the intervals given for these structures by Mitra and Boyer (1986). Duplexes with $u/s = 1$ are a special case of an antiformal stack that only grows vertically, but not in width. Structures with horses that are not imbricated (represented in Fig. 4 by the region labeled *B*) are formed when $l/s < 1-2u/s$, whereas structures with overlapping horses (duplexes and antiformal stacks) form for l/s ratios larger than this value.

The formation of duplexes with a planar roof thrust, which are common in nature, can be simulated successfully if we use a transformation where the displacement length is constant and parallel to the active fault surface. Attempts by previous workers, on the other hand, which

assumed constant bed thickness and bed length, resulted in corrugated roof thrusts. It is not possible to form a duplex with a planar roof thrust and preserve forelimb thickness under flexural slip parallel to the active fault. The topology of the axial planes delimiting the forelimbs of the horses (for example axial plane III in Fig. 3a) controls whether the roof thrust becomes truly planar or not. In models with constant bed thickness and bed length, these axial planes bisect the angles formed by the dip domains of the hanging wall. In our model, on the other hand, the axial planes delimiting the forelimbs of the horses are parallel to the plane that bisects the angle between the roof thrust and the ramp (Figs 2 & 3a).

Furthermore, we show that the location of duplexes with a perfectly planar roof thrust in a u/s vs l/s diagram is limited to specific straight lines. Duplexes with a perfectly planar roof thrust and small displacements ($u<l$) are located on the vertical line $u/s=1/2$ and on a family of straight lines that intersects the u/s axis at one and has a slope of $(1-n)$, where n is the minimum number of horses required. Duplexes with a perfectly planar roof thrust and large displacements ($u>l$), on the other hand, are located on the line $u/s+l/s=1$ and on a family of straight lines that intersects the u/s axis at $(n-1)/n$.

We also show that the formation of duplexes with a planar roof thrust is independent of the dip or internal geometry of the ramps, whereas most former duplex models were limited to a specific dip or range of dips of the ramps.

Acknowledgements—We acknowledge the reviews by Peter Geiser and Mark McNaught and the comments by David Anastasio. This study has been financially supported by Geological Society of America research grant 4768-91 (to J. C.) and by the National University of Mexico (UNAM).

REFERENCES

Boyer, S. E. and Elliott, D. (1982) Thrust systems. *American Association of Petroleum Geologists Bulletin* **66**, 1196–1230.

Contreras, J. (1991) Kinematic modeling of cross-sectional deformation sequences by computer simulation: coding and implementation of the algorithm. *Computers and Geosciences* **17**, 1197–1217.

Contreras, J. and Suter, M. (1990) Kinematic modeling of cross-sectional deformation sequences by computer simulation. *Journal of Geophysical Research*, **95**, 21,913–21,929.

Cruikshank, K. M., Neavel, K. E. and Zhao, G. (1989) Computer simulation of growth of duplex structures. *Tectonophysics* **164**, 1–12.

De Paor, D. G. (1994) Modeling displacement and deformation in a single matrix operation. *Journal of Structural Geology* **16**, 1033–1037.

Elliott, D. and Johnson, M. R. W. (1980) Structural evolution in the northern part of the Moine thrust belt, NW Scotland. *Transactions of the Royal Society of Edinburgh: Earth Science* **71**, 69–96.

Foley, J. D. and van Dam, A. (1982) *Fundamentals of Interactive Computer Graphics*. Addison–Wesley, Reading, Massachusetts.

Groshong, R. H. and Usdansky, S. I. (1988) Kinematic models of plane-roofed duplex styles. *Geological Society of America Special Paper* **222**, 197–206.

Hardy, S. (1995) A method for quantifying the kinematics of fault-bend folding. *Journal of Structral Geology* **17**, 1785–1788.

Johnson, A. M. and Berger, P. (1989) Kinematics of fault-bend folding. *Engineering Geology* **27**, 181–200.

Liu, S. and Dixon, J. M. (1995) Localization of duplex thrust-ramps by buckling: analog and numerical modelling. *Journal of Structural Geology* **17**, 875–886.

Mitra, G. and Boyer, S. E. (1986) Energy balance and deformation mechanisms of duplexes. *Journal of Structural Geology* **8**, 291–304.

Mitra, S. (1986) Duplex structures and imbricate thrust systems: geometry, structural position, and hydrocarbon potential. *American Association of Petroleum Geologists Bulletin* **70**, 1087–1112.

Shi, Y. and Wang, C.-Y. (1987) Two-dimensional modeling of the *P–T–t* paths of regional metamorphism in simple overthrust terrains. *Geology* **15**, 1048–1051.

Suppe, J. (1983) Geometry and kinematics of fault-bend folding. *American Journal of Science* **283**, 684–721.

Suppe, J. and Namson, J. (1979) Fault-bend origin of frontal folds of the western Taiwan fold-and-thrust belt. *Petroleum Geology of Taiwan* **16**, 1–18.

Tanner, P. W. G. (1992) The duplex model: implications from a study of flexural-slip duplexes. In *Thrust Tectonics*, ed. K. R. McClay, pp. 201–208. Chapman and Hall, London.

Truesdell, C. and Toupin, R. (1960) The classical field theories. In *Encyclopaedia of Physics*, ed. S. Flugge, Vol. 3, pp. 226–793. Springer-Verlag, New York.

Twiss, R. J. and Moores, E. M. (1992) *Structural Geology*. W. H. Freeman and Company, New York.

APPENDIX

Strain analysis

The inhomogeneity of the displacement vector field across axial planes causes an internal deformation of the stratigraphic layering by simple shear. The quadratic elongation λ of an arbitrary material line of the model, after having passed through m fault segments, can be expressed as

$$\lambda = (\cos\delta + \gamma_T \sin\delta)^2 + \sin^2\delta, \tag{A1}$$

where δ is the initial orientation (measured counterclockwise) of the line with respect to the x-axis and γ_T is the shear strain induced by the transformation, which is given by

$$\gamma_T = \tan\psi + 2\sum_{i=1}^{m} \tan(\alpha_i/2), \tag{A2}$$

where $\tan\psi$ is the external shear applied to the hanging wall (Fig. 2).

The invariant directions (directions of no elongation) are

$$\delta_1 = 0$$
$$\delta_2 = 1/2 \arctan\gamma_T \pm \pi/2 \tag{A3}$$

Note that the first invariant direction coincides with the slip direction. Similarly, the orientation δ' of an arbitrary material line after having

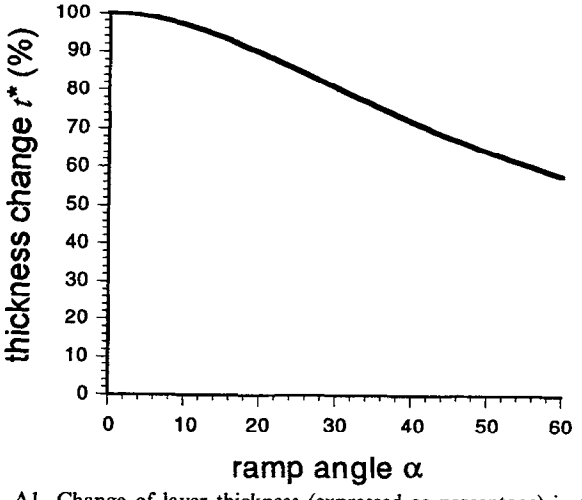

Fig. A1. Change of layer thickness (expressed as percentage) in the forelimb of a fault-related fold resulting from fault-parallel transport over a single ramp, without application of external simple shear.

passed through m fault segments can be expressed as

$$\delta' = \arctan\left(\frac{\sin\delta}{\cos\delta + \gamma_T \sin\delta}\right) + \sum_{i=1}^{m} \alpha_i, \tag{A4}$$

where the first term on the right side of the equation represents the rotation caused by the external simple shear and $\Sigma\alpha_i$ passive rotations induced by the transport of the line across the fault inflections (Fig. 2). Equations (A1) to (A4) are more general expressions of equations presented in Contreras and Suter (1990).

The forelimb thickness of the horses does not remain preserved under flexural slip parallel to the active fault; a layer with stratigraphic thickness t changes its thickness in the forelimb to t^*. This change in thickness can be calculated as follows (fig. 11 in Contreras and Suter, 1990):

$$t^* = t' \cos\eta \tag{A5}$$

where t' is given by

$$t' = t(\lambda_T^{1/2} + 1) \tag{A6}$$

and η by

$$\eta = \delta'_T + \delta' - \pi/2, \tag{A7}$$

where λ_T is the quadratic elongation in the direction $\delta_T = \delta - \pi/2$, perpendicular to the stratigraphic layering of the forelimb with dip δ. Figure A1 shows this change in thickness for the special case of a single ramp and no external simple shear.